Antiviral Research 168 (2019) 121–127

Contents lists available at ScienceDirect

Antiviral Research

journal homepage: www.elsevier.com/locate/antiviral

Dual targeting of dengue virus virions and NS1 protein with the heparan sulfate mimic PG545

Naphak Modhiran[a,b], Neha S. Gandhi[c], Norbert Wimmer[a,b], Stacey Cheung[a,b], Katryn Stacey[a,b], Paul R. Young[a,b], Vito Ferro[a,b,*], Daniel Watterson[a,b,*]

[a] School of Chemistry and Molecular Bioscience, The University of Queensland, Brisbane, Australia
[b] Australian Infectious Diseases Research Centre, The University of Queensland, Brisbane, Australia
[c] School of Mathematical Sciences and Institute of Health and Biomedical Innovation, Queensland University of Technology, Brisbane, Australia

ARTICLE INFO

Keywords:
DENV
NS1
Heparan sulfate
Vascular leakage
Cytokine activation
Mouse model

ABSTRACT

Dengue virus (DENV) is the most prevalent mosquito-borne flavivirus that infects humans. At present, there are no specific antiviral drugs to treat DENV infection and vaccine development has met with challenges. DENV encodes two glycosaminoglycan (GAG) binding proteins; Envelope (E) and non-structural protein 1 (NS1). While previous work has validated the use of GAG analogues as inhibitors of E mediated virus-cell attachment, their potential for antiviral intervention in NS1 protein toxicity has not yet been explored. Here, we investigate the potential of the heparan sulfate mimetic PG545 as a dual purpose compound to target both DENV virion infectivity and NS1 function. In comparison to a non-sulfated analogue, we show that PG545 potently inhibits DENV infectivity with no cytotoxic effect. Against NS1, PG545 completely blocks the induction of cellular activation and abolishes NS1-mediated disruption of endothelial monolayer integrity. Furthermore, PG545 treatment moderately improves survival from lethal DENV challenge in a murine model. At peak disease, PG545-treated mice have lower viremia, circulating NS1 and serum TNF-α. Consistent with anti-NS1 activity, PG545 treatment also reduces systemic vascular leakage caused by DENV infection *in vivo*. Taken together, these findings demonstrate that the dual targeting of DENV virions and NS1 using GAG analogues offers a new avenue for DENV drug development.

1. Introduction

Mosquito-borne flaviviruses, which include dengue virus (DENV), West Nile virus (WNV), Yellow fever virus (YFV), tick-borne encephalitis (TBEV), Japanese encephalitis (JEV) and the recently emerging Zika virus (ZIKV) are a significant cause of morbidity and mortality worldwide. In the case of DENV, an estimated 390 million infections occur annually, with more than 90 million of these being clinically apparent (Bhatt et al., 2013). In the most severe cases, clinical deterioration is characterized by a thrombocytopenia and vascular leakage syndrome resulting in hemoconcentration, plural effusions and shock. An effective targeted treatment strategy is not available and fluid replacement remains the only approach to clinically manage disease outcome.

DENV genome encodes three structural proteins: capsid (C), membrane protein (M) and envelope protein (E) and seven non-structural proteins (Kuhn et al., 2002). During viral infection, virus absorption is initiated by binding of E protein to cellular receptors and/or attachment factors present on the host cell membrane. While the primary DENV receptor/s is/are yet to be confirmed, there is strong evidence that DENV utilizes sulfated glycosaminoglycans (GAGs), including heparan sulfate (HS), as initial attachment factor(s). HS is a repeating, highly negatively-charged linear co-polymer composed of variably sulfated uronic acid and glucosamine residues and is abundantly expressed on several cell types (Kjellen and Lindahl, 1991). The sulfate groups facilitate virion binding through electrostatic interactions with basic surface residues on the DENV E protein. Several putative GAG binding sites have been previously identified within E, mostly located within domain III (Roehrig et al., 2013; Watterson et al., 2012). The E-GAG interaction provides an attractive target for antiviral development and a growing list of anti-DENV HS mimetics have been trialed *in vitro* (De La Guardia and Lleonart, 2014). The semi-synthetic PI-88 is the only such compound validated in a murine DENV challenge model where it showed an improved average survival time when delivered prior to virus inoculation (Lee et al., 2006).

In addition to E, flaviviruses encode another GAG interacting

* Corresponding authors. School of Chemistry and Molecular Biosciences, The University of Queensland, Brisbane, Australia.
E-mail addresses: v.ferro@uq.edu.au (V. Ferro), d.watterson@uq.edu.au (D. Watterson).

https://doi.org/10.1016/j.antiviral.2019.05.004
Received 25 January 2019; Received in revised form 16 April 2019; Accepted 9 May 2019
Available online 11 May 2019
0166-3542/ © 2019 Published by Elsevier B.V.

protein, non-structural protein 1 (NS1). NS1 is a multifunctional protein essential for viral replication (Watterson et al., 2018). Unlike other non-structural viral proteins, NS1 is secreted from infected cells and is present in patient sera at high levels (Libraty et al., 2002). Secreted NS1 is a key biomarker for diagnosis (Young et al., 2000) and levels have been correlated with disease severity (Libraty et al., 2002). NS1 binds strongly to cell surface GAGs, although no functional relevance has yet been attributed to this interaction (Avirutnan et al., 2007). Recently, we showed that NS1 engages Toll-like receptor 4 (TLR4) on monocytes, resulting in the induction of pro-inflammatory cytokines and chemokines (Modhiran et al., 2015, 2017). NS1 also acts through TLR4 on endothelial cells to directly disrupt vascular integrity, leading to the hallmark of severe dengue disease, capillary leak. Notably, TLR4 antagonists or anti-NS1 antibodies reduce DENV-induced pathologies in mouse models (Beatty et al., 2015; Modhiran et al., 2015), highlighting the potential of NS1 as an antiviral target.

In view of the previously identified role for GAGs in NS1 binding to cells, we hypothesized that HS mimetics may block NS1 function and therefore provide an alternative strategy for anti-DENV treatment. Such an approach could in theory provide blockade of both virus entry and NS1 engagement with host cells, with the dual outcome of preventing infection and reducing systemic NS1 effects. Here we examine the potential for this approach, using the synthetic HS mimetic PG545 to probe anti-DENV and anti-NS1 activities *in vitro* and *in vivo*.

2. Materials and methods

2.1. Reagents

PG545 is a fully sulfated tetrasaccharide with a cholestanol aglycon (Fig. 1A). PG545 and its non-sulfated precursor, cholestanyl β-maltotetraoside (compound **2**), were prepared according to the literature (Ferro et al., 2012). Maltotetraose persulfate (compound **3**) was also prepared according to the literature (Parish et al., 1999). PG545 was solubilized in either phosphate buffered saline (PBS) (for *in vivo* and anti-NS1 assays) or dimethyl sulfoxide (DMSO) (for antiviral assays), and compound **2** and **3** were solubilized in DMSO and PBS, respectively. Insect-derived NS1 was prepared as described in published work (Modhiran et al., 2015) and supplementary 1S. Ultrapure lipopolysaccharide (LPS) from *E.coli* 0111:B4 strain was purchased from Invivogen, USA.

2.2. Cell lines and primary cell culture, virus stock and quantification

Vero (African green monkey) cells, human microvasculature endothelial cells (HMEC-1) and *Aedes albopictus* cells (C6/36) were used in this study. Virus strains used were dengue virus-2 (DENV-2) East Timor strain (ET-300; Genbank EF440433.1), and mouse-adapted DENV strain, D220 (kindly provided by Dr. Eva Harris, School of Public Health, University of California, Berkeley, USA). More details are available in the supplementary materials and methods 2S. Virus titers were determined using an immunoplaque protocol as previously described (Li et al., 2018).

2.3. Plaque reduction neutralisation test (PRNT)

PRNT assays were performed as per the viral titration assay, with the following changes. Compounds were titrated in serum free Optimem (Invitrogen, USA) supplemented with 2% DMSO in round bottom 96 well plates (Nunc, USA). Virus was added at a 1:1 vol ratio to compounds for a final concentration of 2000 plaque forming units (PFU)/ml and virus-compound mixture was incubated for 1 h at 37 °C prior to addition to cells at 50 µl/well. After 1 h virus and compound mixture was removed from cells and overlay added before proceeding as per the immunoplaque assay. IC_{50} values were derived from a three-parameter dose response curve fit to plaque numbers obtained for compound titration performed in duplicate.

2.4. Cytotoxicity assay

The cytotoxicity of PG545, compound **2** and **3** for Vero cells was measured using the MTT assay [3-(4,5-dimethyl-2-thiazolyl)-2,5-diphenyl-2H-tetrazolium bromide]; Sigma, USA) in 96-well plate format as described in (Faddy et al., 2016).

2.5. Human peripheral blood mononuclear cells (PBMCs) activation assay

PBMCs were isolated from buffy coats of anonymous donors (Australian Red Cross Blood Service, Kelvin Grove, Queensland, Australia) by density centrifugation using Ficoll-Paque Plus (GE Healthcare, UK) and cultured in RPMI-1640 supplemented with 2 mM L-glutamine, 10% foetal calf serum (FCS), 100 U/ml penicillin, and 100 µg/ml streptomycin. Cells were seeded at 70,000 cells per well in 96 well-plates and incubated with compounds for 1 h at 37 °C prior to adding NS1 (10 µg/ml).

2.6. Quantification of IL-6 and TNF-α

Supernatants of treated cells were harvested at 24 h post treatment. For mouse experiments, serum or EDTA-stabilised plasma were collected. Human IL-6 and TNF-α production was quantified by ELISA (R & D Systems, USA) and mouse IL-6 and TNF-α by Ready-SET-Go! ELISA kits (Invitrogen, USA). The procedures were performed according to the manufacturers' protocols.

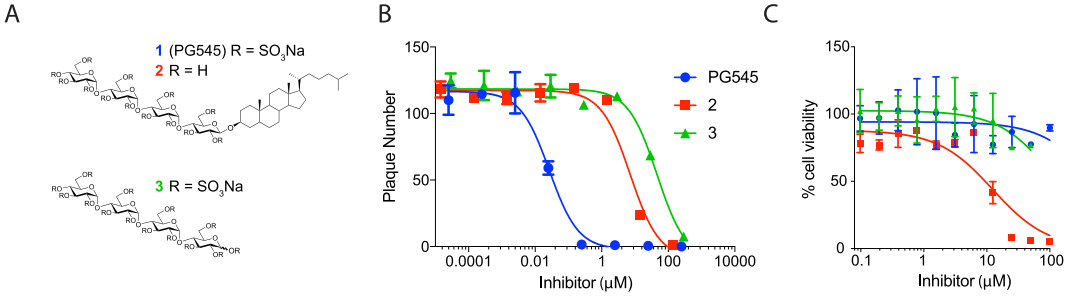

Fig. 1. *In vitro* evaluation of direct antiviral potency and cytotoxicity of PG545 and control compounds. (A) Structures of PG545 (**1**), its analogous non-sulfated precursor (**2**) and sulfated tetrasaccharide (**3**). (B) PRNT activities of PG545 (blue), compound **2** (red) and **3** (green) were determined using Vero cells. Virus was added at a 1:1 vol ratio to compounds for a final concentration of 2000 PFU/ml with 1% DMSO at highest concentration of PG545 or compound **2**, and virus-compound mixture was incubated for 1 h at 37 °C prior to addition to cells at 50 µl/well. (C) Cytotoxicity of compounds to Vero cells. Various concentrations of PG545, compound **2** and compound **3** were incubated with Vero cells for 3 days before assessing cytotoxicity using MTT assay. Shown are the mean and range from 3 independent experiments performed in duplicate with non-linear regression fitting curves.

2.7. Trans endothelial electrical resistance (TEER) measurement

TEER assay was performed as previously described (Modhiran et al., 2015). Confluent HMEC-1 cells were incubated with NS1 (10 μg/ml) or PG545 or a mixture of PG545 and NS1. Endothelial permeability was evaluated over 24 h by measuring trans-endothelial electrical resistance (TEER) using the EVOM2 epithelial voltohmmeter (World Precision Instruments, USA). Relative TEER was expressed as the ratio of resistance value as follows: [Ω (experimental condition) – Ω (medium alone)]/[Ω (untreated cells) – Ω (medium alone)].

2.8. Mouse challenge and treatment

Mouse experiments were performed with the approval of the University of Queensland Animal Ethics Committee. Eight to ten weeks old AG129 mice, which lack receptors for type I and II IFN (IFN-α/β/γ), were bred at the University of Queensland. Mouse-adapted DENV-2 strain D220 was delivered intraperitoneally (i.p.) at 5×10^5 PFU/mouse. Mice were administered with PG545 (20 mg/kg) or PBS control via intravenous (i.v.) injection every two days, starting either 1 h prior or 2 days post infection (dpi). Mice were monitored for morbidity (scored 0–9), weighed daily and recorded as deceased the following day if they were euthanized due to a morbidity score of 9 or lost more than 15% of their initial weight. Mice were monitored for clinical sign of illness (i.e. ruffled fur, stiffness, hunch and loss of appetite) and weight at least once a day for the duration of the experiment.

2.9. Systemic vascular leakage assessment

Vascular leakage was quantified with Evans Blue dye as previously described (Modhiran et al., 2015). Briefly, at 4 dpi 200 μl of freshly prepared 5 mg/ml Evans blue dye was injected i.v. and allowed to circulate for 2 h before mice were anaesthetised and extensively perfused with PBS. Tissues were collected in pre-weighed tubes containing 1 ml N,*N*-dimethylformamide and incubated at 37 °C for 24 h. Extracted Evans Blue was assessed by measuring OD610 in samples, in comparison with a standard curve. Data was expressed as ng Evans Blue dye/mg tissue weight.

2.10. Molecular docking of heparin tetrasaccharide and PG545 with NS1

The crystal structure of full-length glycosylated DENV NS1 (PDB: 4O6B) lacks the flexible wing loop (Akey et al., 2014). The missing region of the flexible loop was modelled based on the crystal structure of the membrane association domain of Zika virus NS1 (PDB: 5K6K) (Brown et al., 2016). The modelled full-length DENV NS1 structure was subsequently used for molecular docking studies. The binding site for heparin tetrasaccharide on the surface of DENV NS1 dimeric structure was predicted using ClusPro heparin tetrasaccharide dp4 docking protocol (Mottarella et al., 2014). The blind docking process was performed for prediction of interaction between DENV NS1 and PG545 ligand using Swiss-dock and PatchDock web-servers (Grosdidier et al., 2011). PLIP webserver was used to analyse the protein-PG545 interactions (Salentin et al., 2015). Molecular dynamics (MD) simulation between NS1 dimer and PG545 complex obtained from docking studies was performed using pmemd.cuda of AMBER16. The residues forming the binding site for PG545 were investigated using PLIP (Salentin et al., 2015). See supplementary 3S for more details.

2.11. Surface plasmon resonance analysis of PG545-NS1 interaction

Surface plasmon resonance (SPR) measurements were performed using a Biacore T200 instrument (GE Healthcare, USA). Purified NS1 was immobilized on CM5 Series Sensor Chip using EDC/NHS coupling (GE Healthcare, USA). The final captured response units of NS1 was 10,105 RU. Binding of PG545 to NS1 was tested using a Multi-Cycle High Performance Kinetics assay. Multiple concentrations of PG545 (370 nM–30 μM) were injected over the chip surface, followed by regeneration between each concentration. Each concentration was injected for 300 sec followed by a dissociation period of 600 sec. The chip surface was regenerated between each cycle using Glycine pH 1.7 (GE Healthcare, USA). A control flow cell that was prepared as above but without the addition of NS1 was used for reference subtraction.

2.12. Statistics

All data were analysed using GraphPad Prism version 7 (GraphPad Software, La Jolla, CA, USA). The IC_{50} and CC_{50} value derived from a three-parameter dose responses curve fit were assessed at 95% confidence interval (CI). Differences among groups were examined using One-way ANOVA (Sidak's test) or Two-way ANOVA using Tukey's test. $P \leq 0.05$ (*), $P \leq 0.01$ (**), $P \leq 0.001$ (***), $P \leq 0.001$ (****) were considered statistically significant.

3. Results

3.1. In vitro activity of PG545 and derivatives against DENV

PG545 consists of a fully charged sulfated tetrasaccharide (as a HS mimetic) linked to a lipophilic sterol moiety (Ferro et al., 2012). To probe the individual activities of these two components we investigated the antiviral potency of compounds representing the lipidic and charged components of PG545 in isolation, including the non-sulfated tetrasaccharide steroid conjugate (**2**) and the sulfated tetrasaccharide lacking the steroid (**3**) (Fig. 1A). Serial dilutions of PG545, compound **2** and compound **3** were pre-incubated with virus for 1 h before adding to cells. As shown in Fig. 1B, the antiviral activity of PG545 was significantly higher than that observed for compounds **2** and **3** with IC_{50} values of 26.64 nM (95% CI: 11.2–19.2), 14.13 μM (95% CI: 6.2–11.2) and 90.63 μM (95% CI: 39.5–70.2 μM), respectively. No significant cell viability effects were observed at concentrations of 100 μM for PG545 and compound **3**, whereas compound **2** had a CC50 of 12.4 μM (95% CI: 4.8–8.2 μM) similar to its IC_{50} (Fig. 1C). DMSO was used as vehicle control and at the concentration used (0.4%) showed no toxicity to cells (Fig.S1). Consequently, we conclude that whilst PG545 has substantial capacity for inhibiting DENV infection, without the lipid moiety compound **3** has limited activity, and without sulfation compound 2 is toxic and therefore has no confirmed anti-viral activity.

3.2. In vitro activity of PG545 and derivatives against DENV NS1

Previously, we developed two functional assays to assess NS1 function *in vitro* to probe the two major NS1-induced pathologies, inflammatory cytokine induction and impairment of vascular integrity (Modhiran et al., 2015). Here we applied these assays to assess the potential for HS mimetics to block NS1 function. We observed that PG545 inhibited IL-6 production in NS1 treated PBMCs (Fig. 2A) with an IC_{50} of ~300 nM. In comparison, the charged tetrasacharide (compound **3**) showed only marginal reduction of NS1 activity at both 1 and 10 μM, while the uncharged cholesterol conjugate (compound **2**) did not block NS1-triggered IL-6 at any concentration tested. Notably, IL-6 induction from LPS stimulation, a known TLR4 ligand, was not diminished by any of the compounds, indicating that the observed NS1 inhibition likely occurs through specific interaction between PG545 or compound **3** and NS1 rather than the compounds with TLR4. Additionally, inhibition of NS1-induced endothelial monolayer permeability by PG545 was assessed by TEER assay. We found that PG545 at a concentration of 1 μM, but not 0.1 μM (data not shown), completely blocked NS1-induced hyperpermeability in HMEC-1 cells (Fig. 2B).

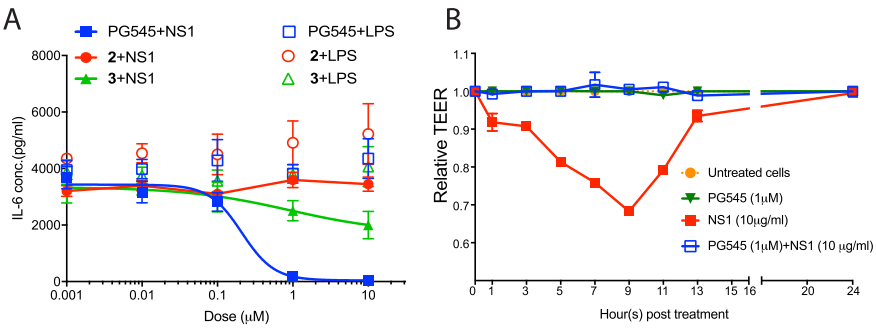

Fig. 2. PG545 strongly and selectively inhibits NS1 activities *in vitro* (A) IL-6 induction by NS1, but not LPS, was inhibited by PG545 in a dose-dependent manner. To assess cell activation, 70,000 cells were preincubated with PG545 or compounds **2** and **3** for 1 h, and NS1 (10 μg/ml) or LPS (10 ng/ml) as indicated. Supernatants were harvested after 24 h for IL-6 quantification. (B) PG545 completely inhibits NS1-induced permeability of an HMEC-1 cell monolayer. Confluent HMEC-1 on transwells were incubated with NS1 (10 μg/ml), PG545 (1 μM) or a premixture of PG545 and NS1. The resistance of HMEC-1 was monitored every 2 h for 24 h. Shown are the mean and range from 2 independent experiments performed in duplicate.

3.3. *In vivo efficacy of PG545 in a lethal dengue mouse model*

We next examined the activity of PG545 in the AG129 mouse model (Orozco et al., 2012). Using a similar dosing strategy to that which had been previously validated in the Ross River virus (RRV) murine model (Supramaniam et al., 2018), mice were administered PG545 at 20 mg/kg (i.v.) from either 1 h prior to infection or 2 dpi, and every second day thereafter (Fig. 3A). As shown in Fig. 3B, PBS-treated infected mice all required culling by day 6 post infection. Notably, both prophylactic and therapeutic treatment with PG545 increased survival on day 10 dpi to 37.5% and 25%, respectively, when compared to those of PBS treatment, although statistical significance of $P < 0.05$ was not met ($P = 0.14$ and 0.19, respectively). Consistent with survival, PG545 treatment resulted in a reduction in symptoms starting from day 4 p.i., compared to PBS-treated infected mice. The therapeutic treatment model showed delayed symptom development and both treatment regimens reduced maximum clinical score compared to control. Symptoms for mice that survived from both treatment groups eventually reduced before levelling-off in overall scores from day 6 and 7 for the pre- and post-treatment, respectively (Fig. 3C). Incomplete recovery was attributed to neurological damage, manifested by loss of equilibrium and head tilt. Treatment also impacted on weight loss, and while both PG545 regimes showed similar initial weight loss kinetics to the control, treated mice that survived did not reach the humane endpoint criterion of 85% experimental starting weight and some recovery was observed for the prophylactic group (Fig. 3D). We also observed a modest but significant reduction in viral load on 3 dpi (Fig. 3E) and circulating NS1 on 3 and 4 dpi (Fig. 2F) in PG545 treated mice compared to those without PG545 treatment. In addition to viral antigens, we observed reduction of IL-6 at 4 dpi for PG545 therapeutically-treated mice, and a significant reduction of TNF-α at 4 dpi for both treatment regimes.

3.4. *Effect of PG545 in DENV-induced systemic vascular permeability*

We next investigated the potential of PG545 to reduce DENV-induced vascular leakage, a key pathology in severe disease. To address this, AG129 were administered with PG545 either prophylactically or therapeutically and vascular leak assessed on day 4 post infection as outlined in Fig. 4A. Infected mice receiving PBS treatment displayed elevated levels of Evans blue dye in the liver (Fig. 4B) and the small intestine (Fig. 4C) compared to uninfected mice, indicative of substantial DENV induced vascular leakage. Infected mice administered PG545 (both pre or post-virus challenge) had lower levels of leakage relative to PBS treated DENV, but the effect only reached statistical significance of $P < 0.05$ for liver samples from the prophylactically treated mice.

3.5. *Prediction of a heparin tetrasaccharide and PG545 binding site on NS1*

To better elucidate the interaction between NS1 and PG545 we performed docking and molecular dynamics analysis. The previously solved crystal structure of the DENV NS1 C-terminal domain revealed a belt of bound sulfate ions at the central dimeric interface of the β-ladder domains (Edeling et al., 2014). When modelled on the full-length hexameric structure of DENV NS1 (Fig. S2A) this region is surface exposed and therefore a potential binding site for ligands of anionic character, including sulfated GAGs. Docking calculations using heparin tetrasaccharide model probes demonstrated the electrostatic patch consisting of residues Lys101, Lys174, Gln175, Lys189, Lys245, Lys227, Trp232 and Asn234 as the main feature of the putative heparin binding site (Fig S2B). Besides the basic residues from the β-ladder, residues from the hydrophobic β-roll and connector segment such as Lys9, Lys11, Lys14 and His26 were also predicted to interact with heparin tetrasaccharide. Docking calculations of PG545 using two distinct programs PatchDock and Swissdock identified similar binding sites on the surface of the DENV NS1 dimer. Two molecules of PG545 were predicted to bind to two identical and symmetrical sites on the DENV NS1 dimer, and are positioned on the outside face of the hexamer form (Fig.S2C). The free energy of binding of the pose selected from Swissdock is −13.6 kcal/mol. As shown in Fig. 5A, in this arrangement the PG545 sulfates form salt-bridge interactions with basic NS1 surface residues including Lys172, Lys174, His224, Lys227 and Lys245, whereas the cholestenol aglycon formed hydrophobic contacts with Glu154, Glu156, Asp157 and Leu206. Hydrogen bonds of the ligand were observed with the side-chains of residues Gln253, Asn234, Ser228, Thr209, Ser181, Asp176 and Glu154 (Fig. 5B). Overall, these results indicate that GAG-NS1 interactions may involve multiple sites spanning more than one domain.

3.6. *SPR analysis of PG545 binding to NS1*

SPR was used to assess direct binding of PG545 to NS1 protein. Approximately 10000 RU of purified NS1 was immobilized on a CM5 chip and a range of PG545 concentrations injected over multiple cycles to establish binding kinetics, with a blank cell used to control for background binding of PG545 to the chip surface. A dose dependent signal was observed in the NS1 immobilized flow cell, consistent with a direct interaction between PG545 and NS1 (Fig. 5C). Sensorgrams were fitted with a 1:1 binding model (Biacore T200 Software) and binding parameters with standard error were derived from the fitted model: k_a 4596 ± 25 ($M^{-1}s^{-1}$), k_d 316.4 ± 1.4 × 10^{-5} (s^{-1}) and Kd 688 ± 5 nM.

4. Discussion

The use of soluble GAGs and GAG-mimetics as potential anti-flaviviral drugs has been well established within the literature. Indeed, HS and related GAG molecules have long been recognized attachment factors for a wide range of flaviviruses (Germi et al., 2002), including DENV (Chen et al., 1997; Kroschewski et al., 2003; Su et al., 2001). Despite this knowledge, few GAG-based inhibitors have been tested in pre-clinical models of DENV disease and none have progressed to clinical trials. PG545 was initially developed for cancer treatment,

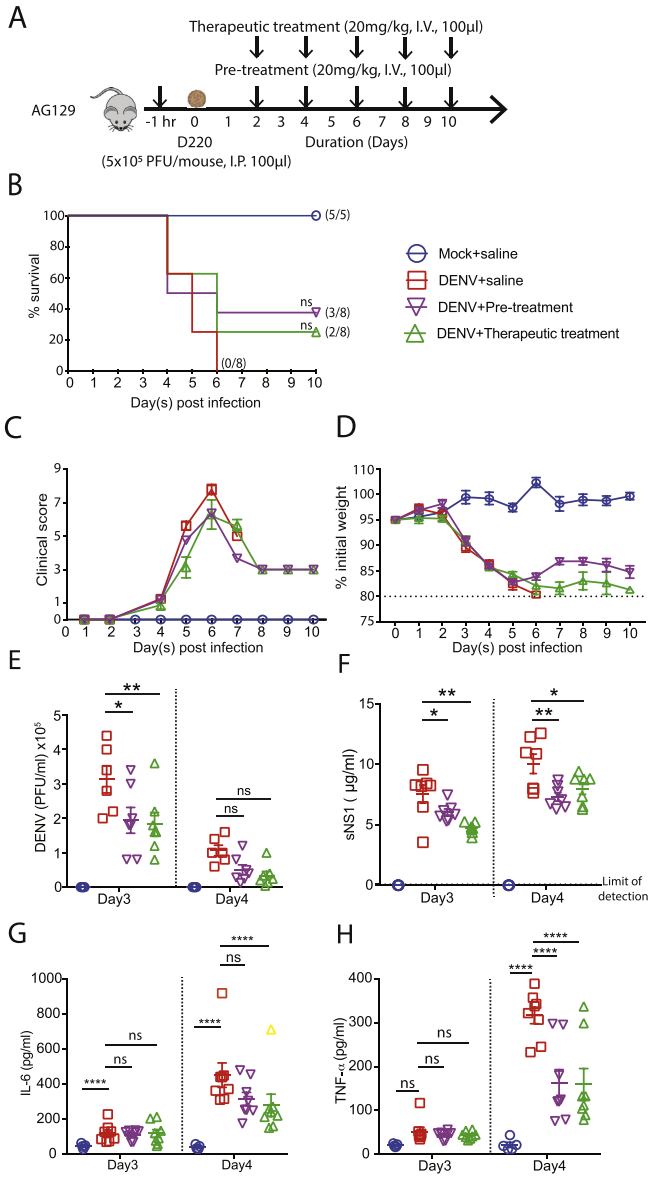

Fig. 3. Antiviral efficacy of PG545 in lethal mouse models of DENV infection. (A) Experimental timeline for testing PG545 efficacy. Nine to ten-week old male AG129 mice were administered with PG545 (20 mg/kg; 100 µl; i.v. 1 h prior (pre-treatment) to or 2 dpi (therapeutic treatment) or saline as control vehicle. Mice were inoculated with 5×10^5 PFU/mouse (100 µl; i.p.) or saline as mock control. Mice were administered PG545 every 2 days for the duration of the experiment. (B) Survival curve, (C) clinical score, (D) weight loss were monitored. (E-H) Blood were collected on day 3 and 4 after infection for quantification of viral load (E), circulating NS1 (F), IL-6 (G) and TNF-α (H). Data are expressed as mean ± SEM from N = 8 (DENV, pre-treatment and therapeutic treatment) and N = 5 (mock). Two outlier were identified by Grubb's test (α = 0.05) and statistical significant was only achieved when they were excluded from analysis; orange square (DENV + saline) and yellow triangle (DENV + therapeutic treatment). The asterisk indicates a difference that is statistically significant (*$P < 0.05$, **$P < 0.001$ and ****$P < 0.001$).

where it has been validated in preclinical animal models and successfully applied in a phase I clinical trial for advanced solid tumours (Dredge et al., 2018). The potential for repurposing PG545 as an antiviral agent has been previously investigated, with efficacy observed against respiratory syncytial virus (RSV) (Lundin et al., 2012), herpes simplex virus (HSV) (Said et al., 2016), human immunodeficiency virus (HIV) (Said et al., 2010) and RRV (Supramaniam et al., 2018). In the present study, we examined a similar mode of viral inhibition for DENV. Two additional compounds were chosen for evaluation of their anti-DENV activity *in vitro*, representing the charged and lipophilic components that make up the unique PG545 structure. As expected, the direct antiviral potency of PG545 far exceeds the effects of the two control compounds. Both the charged tetrasaccharide (**3**) and unsulfated steroid conjugate (**2**) had similar IC_{50} values. However, while the modest antiviral effect of compound **3** is likely due to competition of GAG-virus binding, the activity of the lipophilic compound **2** is likely due to the cytotoxicity of this compound. Consistent with previous studies (Dredge et al., 2011), PG545 was non-toxic, despite the presence of the cholestanol aglycon.

Notably, PG545 was extremely effective against DENV *in vitro* (IC_{50} 25 nM, 63 ng/ml), which was ~50 times more active than that observed against other viruses when tested in a similar assay setup (RSV IC_{50} 2.2 µg/ml, HSV-2 IC_{50} 0.8 µg/ml, RRV IC_{50} 0.4–4.5 µg/ml, HIV-1 IC_{50} 14.4 µg/ml) (Lundin et al., 2012; Said et al., 2010, 2016; Supramaniam et al., 2018). The enhanced antiviral effect may be driven by the reported ability of soluble cholesterol to readily intercalate and disrupt the DENV virion membrane (Lee et al., 2008). Consistent with this mode of action, the anti-DENV activity we observed is also far greater than that which has been reported for HS and related compounds, which lack an aglycon lipophilic anchor (Kim et al., 2017). It will therefore be of interest to examine whether the binding of PG545 to the DENV virion merely hinders cell attachment or leads to spontaneous viral inactivation through membrane disruption or triggering of the viral fusion mechanisms. The second hypothesis is in line with that previously proposed for HSV-2, where PG545 incubation led to direct virion lysis as assessed by transmission electron microscopy (Said et al., 2016). Further study on the molecular mechanisms that drive the potent anti-DENV activity of PG545 could inform new drug design and offer insight to improve existing E targeting molecules.

In addition to direct antiviral action, our studies reveal that PG545 also acts to inhibit NS1 toxicity *in vitro*, blocking both NS1 induced IL-6 production and NS1 driven disruption of endothelial integrity. Interestingly, NS1 induction of IL-6 in human PBMCs was partly inhibited by compound **3**, suggesting a role for charge-based interactions and NS1 cell attachment. Similar to what we observed in the PRNT assay, PG545 was significantly more active than the charged tetrasacharide component alone, indicating that the lipidic moiety may potentiate PG545-NS1 interaction. *In silico* docking of the tetrasaccharide moiety alone revealed a putative binding site on the outer surface of NS1, located at the central interface between the NS1 monomers and involving charged residues in both the β-ladder and wing domains. This region has been previously identified as a potential sulfated GAG binding site (Edeling et al., 2014). In comparison, while docking identified a similar central binding region for PG545 (Fig. 5), the charged PG545 headgroup instead makes contact with the β-ladder and the steroidal component interacts with the connector and wing domains. SPR analysis of the NS1-PG545 interaction confirmed a direct interaction (Fig. 5C) with a binding affinity (Kd value) of ~700 nM. While the specific sites that underpin the NS1-PG545 interaction remain to be determined empirically, a role for the wing and associated connector domain in GAG binding may explain the lack of success reported for the binding of HS analogues to JEV C-terminus of NS1, which lacks this region (Poonsiri et al., 2018). Alternatively, a role for the lipidic core of the NS1 hexamer with respect to PG545 binding is also possible. However, as the structure of the lipid core is not known, we were unable to address this possibility through a docking approach. Notably, the lipid core has been previously proposed to play a role in hexamer stabilisation (Gutsche et al., 2011). In this case, PG545 may potentially exert anti-NS1 activity by disruption of the NS1 hexamer, although the oligomeric dependence of the NS1-TLR4 interaction remains unknown.

NS1 has also been reported to trigger heparanase activation and HS cleavage which are proposed to be critical in the disruption of endothelial monolayers by NS1 (Glasner et al., 2017). HS cleavage

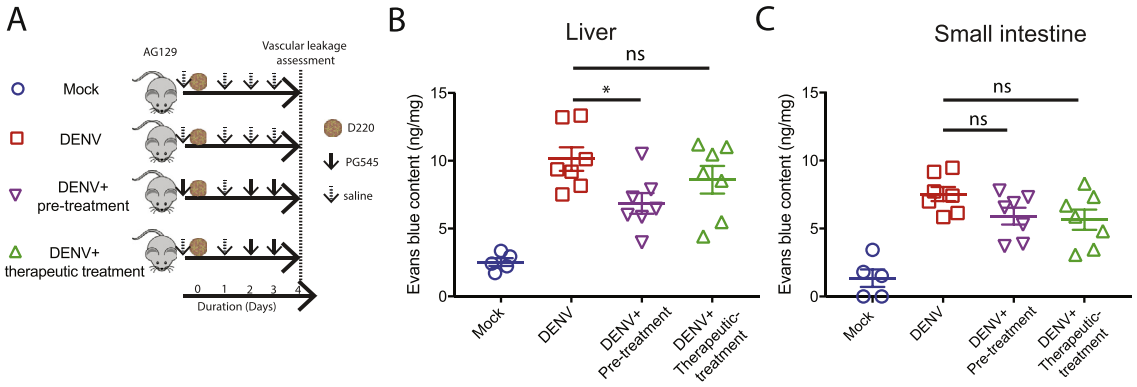

Fig. 4. Effect of PG545 prophylactic and therapeutic treatment on DENV-induced systemic vascular leakage. (A) Experimental timeline; seven to nine-weeks old male AG129 mice were administered with PG545 (20 mg/kg; 100 µl; i.v.) or saline as control vehicle at 1 h prior to or 2 dpi and then as indicated on days 2 and 3. Mice were inoculated with 5×10^5 PFU/mouse (100 µl; i.p.) or saline as mock control. On 4 dpi mice were injected i.v. with Evans blue dye and after 2 h perfused extensively with PBS to allow vascular permeability to be determined. Evans blue extravasation in the (B) liver and (C) small intestine were quantified. Data are expressed as mean ± SEM from N = 7 (DENV, pre-treatment and therapeutic treatment) and N = 5 (mock).

products are in turn reported to trigger the release of pro-inflammatory cytokines in a TLR4-dependent manner (Goodall et al., 2014; Johnson et al., 2002). Therefore, PG545 may block NS1 function indirectly through direct heparanase inhibition (Ferro et al., 2012), thereby reducing downstream IL-6 responses (Fig. 1C). Indeed, recent work has investigated the potential for heparanase inhibition with regard to NS1 induced leak, with modest anti-NS1 effects observed for the small molecule heparanase inhibitor OGT 2115 when used alone, and more potent results when used in combination with sialidase and cathepsin L inhibitors (Glasner et al., 2017; Puerta-Guardo et al., 2016).

Promising results from *in vitro* assays led us to assess PG545 activity in a murine model of disease. We used a 20 mg/kg dose of PG545 that has been previously shown to yield protection in a mouse model of RRV infection (Supramaniam et al., 2018). In agreement with our *in vitro* data, i.v. administration of PG545, delivered either prophylactically or therapeutically, reduced serum viremia and NS1, as well as IL-6 and TNF-α levels in DENV-infected mice. However, only subtle changes in systemic vascular leakage were observed in mice administered PG545, with significant leak reduction only observed in the liver of animals treated prophylactically. These results may underpin the limited survival after treatment we observed in the challenge model. The discrepancies between the modest protection in mice *vs* the potent activity of PG545 against both virus infection and NS1 *in vitro* may be due to complex virus-host interactions that are difficult to mimic in reductionist assay systems. Furthermore, DENV causes thrombocytopenia, platelet dysfunction and coagulopathy and although PG545 has only minimal anti-coagulant activity (Ferro et al., 2012), this effect might be amplified in the DENV infection context. Alternatively, bioavailablity and pharmacokinetic properties of PG545 in DENV-infected mice might be lower than other models (Ferro et al., 2012) and remain to be tested. In light of these data, it would be of interest to determine whether modification of the HS-like moiety could be made to improve antiviral and anti-NS1 activity in a selective manner, and to further probe the mode of action of these compounds by direct NS1 binding, generation of viral escape mutants or investigation of downstream blockage of NS1 induced pathways including heparanse activity.

Current strategies for DENV antiviral development include targeting viral entry and replication as well as host cofactors and inflammatory responses. However, while these approaches have seen some success in preclinical studies, none have been successfully translated to the clinic (Lim et al., 2013; Whitehorn et al., 2014) and new avenues for therapeutic intervention are clearly needed. The recognition of NS1 as a viral toxin provides a new target for drug discovery. In this study, we identified that a HS mimetic could effectively target both DENV infection and NS1 responses *in vitro* and *in vivo*. This represents the first identification of a dual targeting anti-flaviviral drug, and may offer potential to reduce the emergence of viral resistance as has been observed for similar approaches in cancer and microbial drug development (Pokrovskaya and Baasov, 2010). Our results also indicate that the addition of a lipophilic anchor improves both antiviral and anti-NS1 activity, providing a template strategy to improve other E or NS1 targeting antivirals. However, as the observed effectiveness of PG545 *in vivo* was limited, further understanding of molecular mechanisms involved and improvements on activity will be required before progression to clinical phase testing.

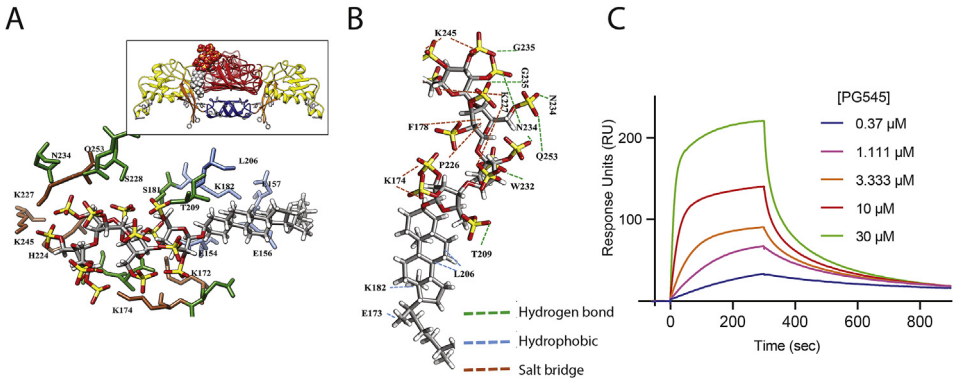

Fig. 5. Binding interactions of DENV NS1 with PG545. (A) The PG545 binding site on DENV NS1 was predicted using Swissdock and MD simulations. Optimal PG545 docking bridges the two monomers within the NS1 dimer and also partially occupies the proposed lipid and heparin binding sites (inset, PG545 in space fill and NS1 dimer in cartoon representation and coloured by domain in red, yellow, blue and orange (Akey et al., 2014)). PG545 is presented in CPK elemental colouring in all panels. The PG545 interacting residues in NS1 are coloured according to PG545 interaction; hydrogen bonds (green), hydrophobic interactions (blue) or salt bridge (brown) in (A) and bond network shown for clarity in (B). (C) SPR analysis of PG545 binding to immobilised NS1 protein. Blank-subtracted sensorgrams of the association and dissociation phases of PG545 on immobilised NS1 are shown across a range of PG545 concentrations.

Acknowledgments

This study was supported in part by funds from the Australian Research Council (DP170104431 to VF) and the National Health and Medical Research Council (APP1109738 to KJS, PRY and DW and APP1162507 to DW, PRY and NM). KJS was supported by NHMRC fellowship. NSG gratefully acknowledges the high performance computing resources provided by the Queensland University of Technology. The authors also acknowledge the facilities, and the scientific and technical assistance of the National Biologics Facility (NBF) at the University of Queensland, in particular Dr Martina Jones. NBF is supported by Therapeutic Innovation Australia (TIA). TIA is supported by the Australian Government through the National Collaborative Research Infrastructure Strategy (NCRIS) program.

Appendix A. Supplementary data

Supplementary data to this article can be found online at https://doi.org/10.1016/j.antiviral.2019.05.004.

References

Akey, D.L., Brown, W.C., Dutta, S., Konwerski, J., Jose, J., Jurkiw, T.J., DelProposto, J., Ogata, C.M., Skiniotis, G., Kuhn, R.J., Smith, J.L., 2014. Flavivirus NS1 structures reveal surfaces for associations with membranes and the immune system. Science 343, 881–885.

Avirutnan, P., Zhang, L., Punyadee, N., Manuyakorn, A., Puttikhunt, C., Kasinrerk, W., Malasit, P., Atkinson, J.P., Diamond, M.S., 2007. Secreted NS1 of dengue virus attaches to the surface of cells via interactions with heparan sulfate and chondroitin sulfate E. PLoS Pathog. 3, 1798–1812.

Beatty, P.R., Puerta-Guardo, H., Killingbeck, S.S., Glasner, D.R., Hopkins, K., Harris, E., 2015. Dengue virus NS1 triggers endothelial permeability and vascular leak that is prevented by NS1 vaccination. Sci. Transl. Med. 7, 304ra141.

Bhatt, S., Gething, P.W., Brady, O.J., Messina, J.P., Farlow, A.W., Moyes, C.L., Drake, J.M., Brownstein, J.S., Hoen, A.G., Sankoh, O., Myers, M.F., George, D.B., Jaenisch, T., Wint, G.R.W., Simmons, C.P., Scott, T.W., Farrar, J.J., Hay, S.I., 2013. The global distribution and burden of dengue. Nature 496, 504–507.

Brown, W.C., Akey, D.L., Konwerski, J.R., Tarrasch, J.T., Skiniotis, G., Kuhn, R.J., Smith, J.L., 2016. Extended surface for membrane association in Zika virus NS1 structure. Nat. Struct. Mol. Biol. 23, 865–867.

Chen, Y.P., Maguire, T., Hileman, R.E., Fromm, J.R., Esko, J.D., Linhardt, R.J., Marks, R.M., 1997. Dengue virus infectivity depends on envelope protein binding to target cell heparan sulfate. Nat. Med. 3, 866–871.

De La Guardia, C., Lleonart, R., 2014. Progress in the identification of dengue virus entry/fusion inhibitors. BioMed Res. Int. 2014, 825039.

Dredge, K., Brennan, T.V., Hammond, E., Lickliter, J.D., Lin, L., Bampton, D., Handley, P., Lankesheer, F., Morrish, G., Yang, Y., Brown, M.P., Millward, M., 2018. A Phase I study of the novel immunomodulatory agent PG545 (pixatimod) in subjects with advanced solid tumours. Br. J. Canc. 118, 1035–1041.

Dredge, K., Hammond, E., Handley, P., Gonda, T.J., Smith, M.T., Vincent, C., Brandt, R., Ferro, V., Bytheway, I., 2011. PG545, a dual heparanase and angiogenesis inhibitor, induces potent anti-tumour and anti-metastatic efficacy in preclinical models. Br. J. Canc. 104, 635–642.

Edeling, M.A., Diamond, M.S., Fremont, D.H., 2014. Structural basis of Flavivirus NS1 assembly and antibody recognition. Proc. Natl. Acad. Sci. U. S. A. 111, 4285–4290.

Faddy, H.M., Fryk, J.J., Watterson, D., Young, P.R., Modhiran, N., Muller, D.A., Keil, S.D., Goodrich, R.P., Marks, D.C., 2016. Riboflavin and ultraviolet light: impact on dengue virus infectivity. Vox Sang. 111, 235–241.

Ferro, V., Liu, L., Johnstone, K.D., Wimmer, N., Karoli, T., Handley, P., Rowley, J., Dredge, K., Li, C.P., Hammond, E., Davis, K., Sarimaa, L., Harenberg, J., Bytheway, I., 2012. Discovery of PG545: a highly potent and simultaneous inhibitor of angiogenesis, tumor growth, and metastasis. J. Med. Chem. 55, 3804–3813.

Germi, R., Crance, J.M., Garin, D., Guimet, J., Lortat-Jacob, H., Ruigrok, R.W., Zarski, J.P., Drouet, E., 2002. Heparan sulfate-mediated binding of infectious dengue virus type 2 and yellow fever virus. Virology 292, 162–168.

Glasner, D.R., Ratnasiri, K., Puerta-Guardo, H., Espinosa, D.A., Beatty, P.R., Harris, E., 2017. Dengue virus NS1 cytokine-independent vascular leak is dependent on endothelial glycocalyx components. PLoS Pathog. 13, e1006673.

Goodall, K.J., Poon, I.K., Phipps, S., Hulett, M.D., 2014. Soluble heparan sulfate fragments generated by heparanase trigger the release of pro-inflammatory cytokines through TLR-4. PLoS One 9, e109596.

Grosdidier, A., Zoete, V., Michielin, O., 2011. SwissDock, a protein-small molecule docking web service based on EADock DSS. Nucleic Acids Res. 39, W270–W277.

Gutsche, I., Coulibaly, F., Voss, J.E., Salmon, J., d'Alayer, J., Ermonval, M., Larquet, E., Charneau, P., Krey, T., Megret, F., Guittet, E., Rey, F.A., Flamand, M., 2011. Secreted dengue virus nonstructural protein NS1 is an atypical barrel-shaped high-density lipoprotein. Proc. Natl. Acad. Sci. U. S. A 108, 8003–8008.

Johnson, G.B., Brunn, G.J., Kodaira, Y., Platt, J.L., 2002. Receptor-mediated monitoring of tissue well-being via detection of soluble heparan sulfate by Toll-like receptor 4. J. Immunol. 168, 5233–5239.

Kim, H.J., Hong, Y.H., Kim, Y.J., Kim, H.S., Park, J.W., Do, J.Y., Kim, K.J., Bae, S.W., Kim, C.W., Lee, C.K., 2017. Anti-heparan sulfate antibody and functional loss of glomerular heparan sulfate proteoglycans in lupus nephritis. Lupus 26, 815–824.

Kjellen, L., Lindahl, U., 1991. Proteoglycans - structures and interactions. Annu. Rev. Biochem. 60, 443–475.

Kroschewski, H., Allison, S.L., Heinz, F.X., Mandl, C.W., 2003. Role of heparan sulfate for attachment and entry of tick-borne encephalitis virus. Virology 308, 92–100.

Kuhn, R.J., Zhang, W., Rossmann, M.G., Pletnev, S.V., Corver, J., Lenches, E., Jones, C.T., Mukhopadhyay, S., Chipman, P.R., Strauss, E.G., Baker, T.S., Strauss, J.H., 2002. Structure of dengue virus: implications for flavivirus organization, maturation, and fusion. Cell 108, 717–725.

Lee, C.J., Lin, H.R., Liao, C.L., Lin, Y.L., 2008. Cholesterol effectively blocks entry of flavivirus. J. Virol. 82, 6470–6480.

Lee, E., Pavy, M., Young, N., Freeman, C., Lobigs, M., 2006. Antiviral effect of the heparan sulfate mimetic, PI-88, against dengue and encephalitic flaviviruses. Antivir. Res. 69, 31–38.

Li, J., Watterson, D., Chang, C.W., Che, X.Y., Li, X.Q., Ericsson, D.J., Qiu, L.W., Cai, J.P., Chen, J., Fry, S.R., Cheung, S.T.M., Cooper, M.A., Young, P.R., Kobe, B., 2018. Structural and functional characterization of a cross-reactive dengue virus neutralizing antibody that recognizes a cryptic epitope. Structure 26, 51.

Libraty, D.H., Young, P.R., Pickering, D., Endy, T.P., Kalayanarooj, S., Green, S., Vaughn, D.W., Nisalak, A., Ennis, F.A., Rothman, A.L., 2002. High circulating levels of the dengue virus nonstructural protein NS1 early in dengue illness correlate with the development of dengue hemorrhagic fever. J. Infect. Dis. 186, 1165–1168.

Lim, S.P., Wang, Q.Y., Noble, C.G., Chen, Y.L., Dong, H.P., Zou, B., Yokokawa, F., Nilar, S., Smith, P., Beer, D., Lescar, J., Shi, P.Y., 2013. Ten years of dengue drug discovery: progress and prospects. Antivir. Res. 100, 500–519.

Lundin, A., Bergstrom, T., Andrighetti-Frohner, C.R., Bendrioua, L., Ferro, V., Trybala, E., 2012. Potent anti-respiratory syncytial virus activity of a cholestanol-sulfated tetrasaccharide conjugate. Antivir. Res. 93, 101–109.

Modhiran, N., Watterson, D., Blumenthal, A., Baxter, A.G., Young, P.R., Stacey, K.J., 2017. Dengue virus NS1 protein activates immune cells via TLR4 but not TLR2 or TLR6. Immunol. Cell Biol. 95, 491–495.

Modhiran, N., Watterson, D., Muller, D.A., Panetta, A.K., Sester, D.P., Liu, L., Hume, D.A., Stacey, K.J., Young, P.R., 2015. Dengue virus NS1 protein activates cells via Toll-like receptor 4 and disrupts endothelial cell monolayer integrity. Sci. Transl. Med. 7 304ra142.

Mottarella, S.E., Beglov, D., Beglova, N., Nugent, M.A., Kozakov, D., Vajda, S., 2014. Docking server for the identification of heparin binding sites on proteins. J. Chem. Inf. Model. 54, 2068–2078.

Orozco, S., Schmid, M.A., Parameswaran, P., Lachica, R., Henn, M.R., Beatty, R., Harris, E., 2012. Characterization of a model of lethal dengue virus 2 infection in C57BL/6 mice deficient in the alpha/beta interferon receptor. J. Gen. Virol. 93, 2152–2157.

Parish, C.R., Freeman, C., Brown, K.J., Francis, D.J., Cowden, W.B., 1999. Identification of sulfated oligosaccharide-based inhibitors of tumor growth and metastasis using novel in vitro assays for angiogenesis and heparanase activity. Cancer Res. 59, 3433–3441.

Pokrovskaya, V., Baasov, T., 2010. Dual-acting hybrid antibiotics: a promising strategy to combat bacterial resistance. Expert Opin. Drug Discov. 5, 883–902.

Poonsiri, T., Wright, G.S.A., Diamond, M.S., Turtle, L., Solomon, T., Antonyuk, S.V., 2018. Structural study of the C-terminal domain of nonstructural protein 1 from Japanese encephalitis virus. J. Virol. 92.

Puerta-Guardo, H., Glasner, D.R., Harris, E., 2016. Dengue virus NS1 disrupts the endothelial glycocalyx, leading to hyperpermeability. PLoS Pathog. 12, e1005738.

Roehrig, J.T., Butrapet, S., Liss, N.M., Bennett, S.L., Luy, B.E., Childers, T., Boroughs, K.L., Stovall, J.L., Calvert, A.E., Blair, C.D., Huang, C.Y., 2013. Mutation of the dengue virus type 2 envelope protein heparan sulfate binding sites or the domain III lateral ridge blocks replication in Vero cells prior to membrane fusion. Virology 441, 114–125.

Said, J., Trybala, E., Andersson, E., Johnstone, K., Liu, L.G., Wimmer, N., Ferro, V., Bergstrom, T., 2010. Lipophile-conjugated sulfated oligosaccharides as novel microbicides against HIV-1. Antivir. Res. 86, 286–295.

Said, J.S., Trybala, E., Gorander, S., Ekblad, M., Liljeqvist, J.A., Jennische, E., Lange, S., Bergstrom, T., 2016. The cholestanol-conjugated sulfated oligosaccharide PG545 disrupts the lipid envelope of herpes simplex virus particles. Antimicrob. Agents Chemother. 60, 1049–1057.

Salentin, S., Schreiber, S., Haupt, V.J., Adasme, M.F., Schroeder, M., 2015. PLIP: fully automated protein-ligand interaction profiler. Nucleic Acids Res. 43, W443–W447.

Su, C.M., Liao, C.L., Lee, Y.L., Lin, Y.L., 2001. Highly sulfated forms of heparin sulfate are involved in Japanese encephalitis virus infection. Virology 286, 206–215.

Supramaniam, A., Liu, X., Ferro, V., Herrero, L.J., 2018. Prophylactic antiheparanase activity by PG545 is antiviral in vitro and protects against Ross river virus disease in mice. Antimicrob. Agents Chemother. 62.

Watterson, D., Kobe, B., Young, P.R., 2012. Residues in domain III of the dengue virus envelope glycoprotein involved in cell-surface glycosaminoglycan binding. J. Gen. Virol. 93, 72–82.

Watterson, D., Modhiran, N., Muller, D.A., Stacey, K.J., Young, P.R., 2018. Plugging the leak in dengue shock. Adv. Exp. Med. Biol. 1062, 89–106.

Whitehorn, J., Yacoub, S., Anders, K.L., Macareo, L.R., Cassetti, M.C., Van, V.C.N., Shi, P.Y., Wills, B., Simmons, C.P., 2014. Dengue therapeutics, chemoprophylaxis, and allied tools: state of the art and future directions. PLoS Neglected Trop. Dis. 8.

Young, P.R., Hilditch, P.A., Bletchly, C., Halloran, W., 2000. An antigen capture enzyme-linked immunosorbent assay reveals high levels of the dengue virus protein NS1 in the sera of infected patients. J. Clin. Microbiol. 38, 1053–1057.